Magnetic, half-metallicity and electronic studies of $Cd_{1-x}Zn_xCr_2Se_4$ chromium selenospinels

Meriem. Bouhbou[*1], Reda. MOUBAH[1], Azzam. BELAYACHI[2] and Hassan. LASSRI[1]

[1] LPMMAT, faculté des Sciences Ain Chock, Université Hassan II de Casablanca, B.P. 5366 Casablanca, Morocco.

[2] LPM, Faculté des Sciences, Université Mohammed V, B.P. 1014 Rabat, Morocco.

meriem49bouhbou@gmail.com

1 – ABSTRACT

We have studied the magnetism of crystalline $Cd_{1-x}Zn_xCr_2Se_4$ spinels with ($0.35 \le x \le 0.55$) under magnetic field up to 15 T. The experimental magnetic moment of Cr, Curie temperature, lattice parameter and exchange integrals were found to decrease with Zn substitution. *Ab-initio* calculations carried out using full potential augmented plane wave (FP-LAPW) method were performed to study the magnetic, and electronic structure using generalized gradient approximation (GGA) and the modified Becke-Johnson (mBJ) to correct the gap's energy. The obtained results were in good agreement with the experimental ones. It is shown that there is a competition between ferromagnetic (FM) and antiferromagnetic (AFM) interactions: the super-exchange mechanism slightly increases the AFM contribution and keeps the FM the dominant mechanism in this range of substitution. From the density of states, we demonstrate that the system keeps the half-metallic state for all compositions with 100% spin polarization. Our results highlight that it is possible to obtain a half-metallic semiconductor with tunable magnetic state which is promising for applications in spintronics.

OBJECTIVES

Synthesis of new materials presenting multi-functional application in technology :
- Spintronics
- Photovoltaics
- Magnetic refrigeration

studying physical properties of materials from theoretical and experimental backgrounds in order to have a solid and a better understanding for different systems

2 – EXPERIENCE

$Cd_{1-x}Zn_xCr_2Se_4$ single crystals were prepared by vapor liquid transport (VLT) technique. The combination of starting materials ASe (A = Cd, Zn) and $CrCl_3$ was placed in a ratio 1:2 with a purity of 99.999 %. The mixture was cold weighed and placed at the end of a silica vial with a nominal growth temperature of 1198 K. A gradient temperature was performed in a way that the tube tip is about 323 K cooler than the area holding the reactive. The oven was inclined by 20% relative to horizontal to simplify the liquid flow from which the crystals form at the tip of the vial, the formed crystals have 4 mm size and were too big to be characterized hence, they were finely grinded to obtain polycrystalline powders. More experimental details about samples preparation were previously reported. $CdCr_2Se_4$ crystallizes in a face-centered cubic lattice with a space group Fd-3m: 227. The Zn^{2+} substitutes Cd^{2+} in the tetrahedral sites A sublattice with a random arrangement and surrounded by Se^{2-}, while Cr^{3+} ions prefer to occupy octahedral sites in the spinel B sublattice surrounded by six (Se^{2-}) ions as shown in figure 2. Magnetic measurements were performed using extraction technique with an external applied field up to 15 T in the temperature window 4.2–147 K.

3- Computational detail

Electronic structure calculations were performed using full-potential linearized augmented plane-waves method based on density functional theory (DFT) as implemented in the package Wien2k. We use mBJ plus GGA for exchange-correlation potential to attain our main DFT computation besides the popular GGA by Perdew, Burke, and Ernzerhof (GGA-PBE) in order to compare both approaches. The calculation was performed with a scalar relativistic approach, the spin-orbit coupling was neglected since it has nearly no influence on our results. The k-points used in the calculations were based on 4 4 4 Monkhorst-Pack scheme, and the harmonic expansion made up to l_{max}= 10 in each of the atomic spheres, with $R_{MT}*K_{max}$ = 7, where R_{MT} is the smallest atomic sphere radius in the unit cell and K_{max} is the magnitude of the largest k vector. The atomic sphere radii were set to R_{MT} (Cd) = 2.47, R_{MT} (Cr) = 2.33 and R_{MT} (Se) = 2.33 Bohr (for x=0) and it does change according to the increment that we choose to be 1/8. The self-consistent calculations were assumed to converge when reaching a convergence of 10^{-4} (Ry) and 10^{-3} (e) in energy and charge respectively. We use lattice parameters calculated from our experience results.

5 – Electronic properties
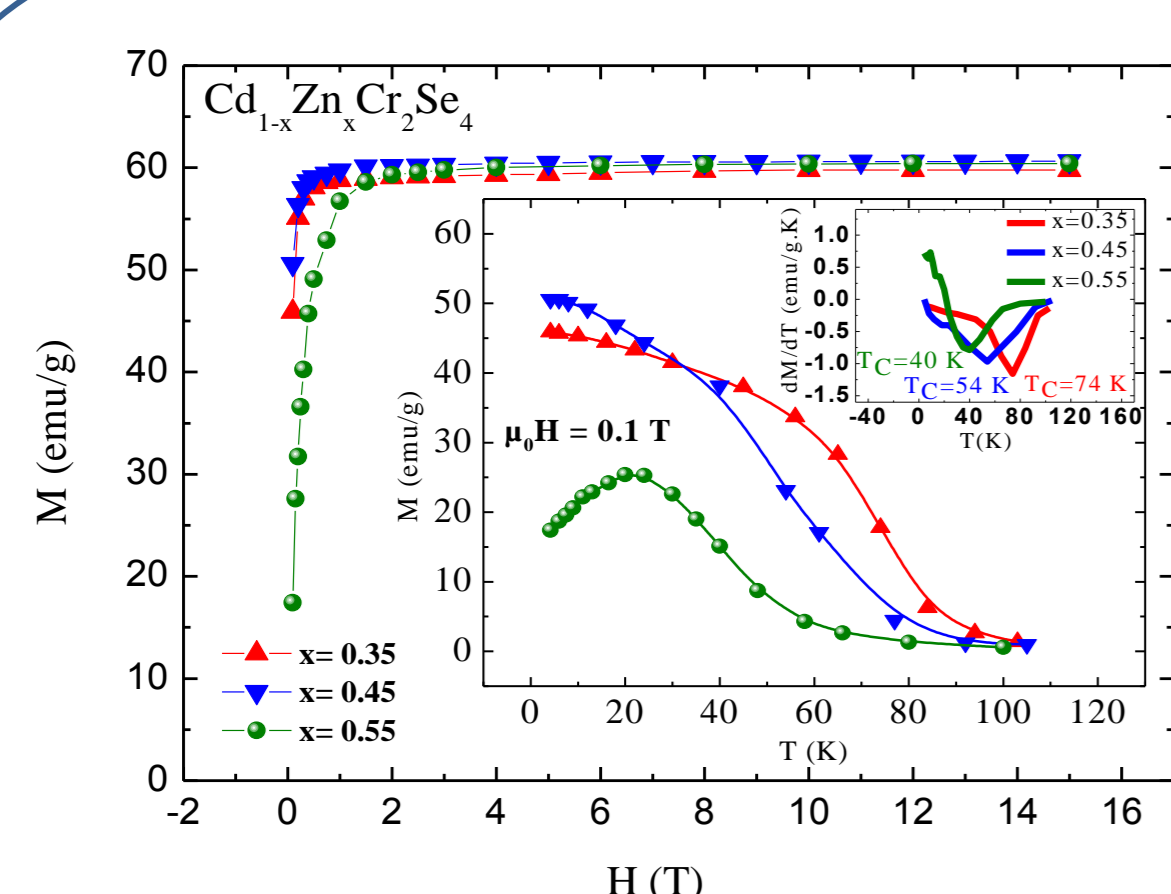

Figure 4 Total (a-c) and partial (d-f) density of states (DOS) calculated with GGA+mBJ approach of $Cd_{1-x}Zn_xCr_2Se_4$ x = 0.125(a), x = 0.375 (b) and x = 0.5 (c). The inset shows the zoom at E_F (left) and partial density of states for Zn-4d, Cd-3d (right).

Figures 4 (d-f) show the partial DOS of the Cr-d, Zn-d, Cd-d and Se-p bands. For all Zn contents, the total DOS for energies around Fermi level (E_F) originate almost from the Cr-d and Se-p orbitals, which permits to obtain a strong spin polarization resulting essentially from the dominated contribution of Cr-3d bands, which is occupied mainly by the majority of spin-up; in contrast the d Cr sub-band of spin down is empty. The strong contribution of the Cr d sub-band of spin-up is due to the hybridization occurred with the Se p states. The low DOS values of Se p band states supports the hybridization effect, the light DOS polarization pointing out a small magnetic moment created at Se atoms (-0.07923 μ_B), while the clear asymmetry of the spectrum suggests a high magnetic moment. Similar performance was shown for all selenospinel samples. However, with Zn substitution the pics broaden and their intensities slightly decrease indicating a tiny decrease of the Cr magnetic moment with Zn content.

4- Magnetic properties

Figure 1: Isothermal magnetization M (H) for $Cd_{1-x}Zn_xCr_2Se_4$ ($0.35 \le x \le 0.55$) samples at T= 4.2 K, the inset displays the change of magnetization as function of temperature under an applied field of 0.1 T with the corresponding curves.
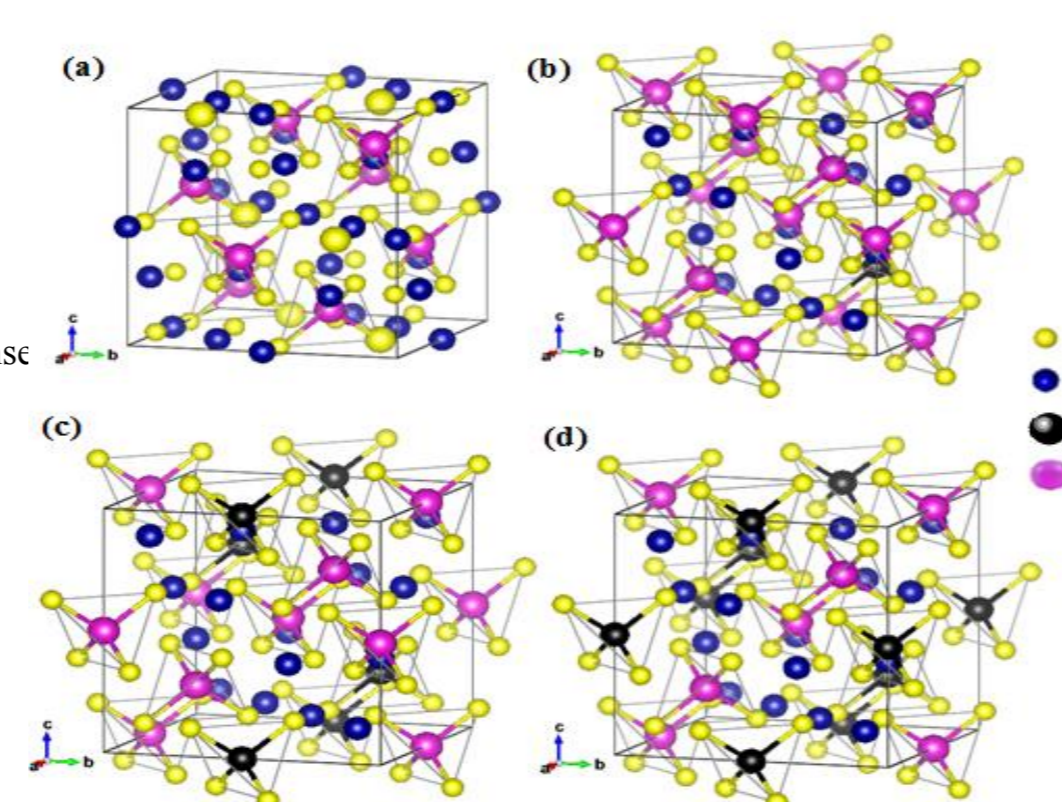
Figure 2: Structure of $Cd_{1-x}Zn_xCr_2Se_4$ for (a) x=0 "Fd-3m: 227" (b) x=0.125 (c) x=0.375 and (d) x=0.5 "1_P1".
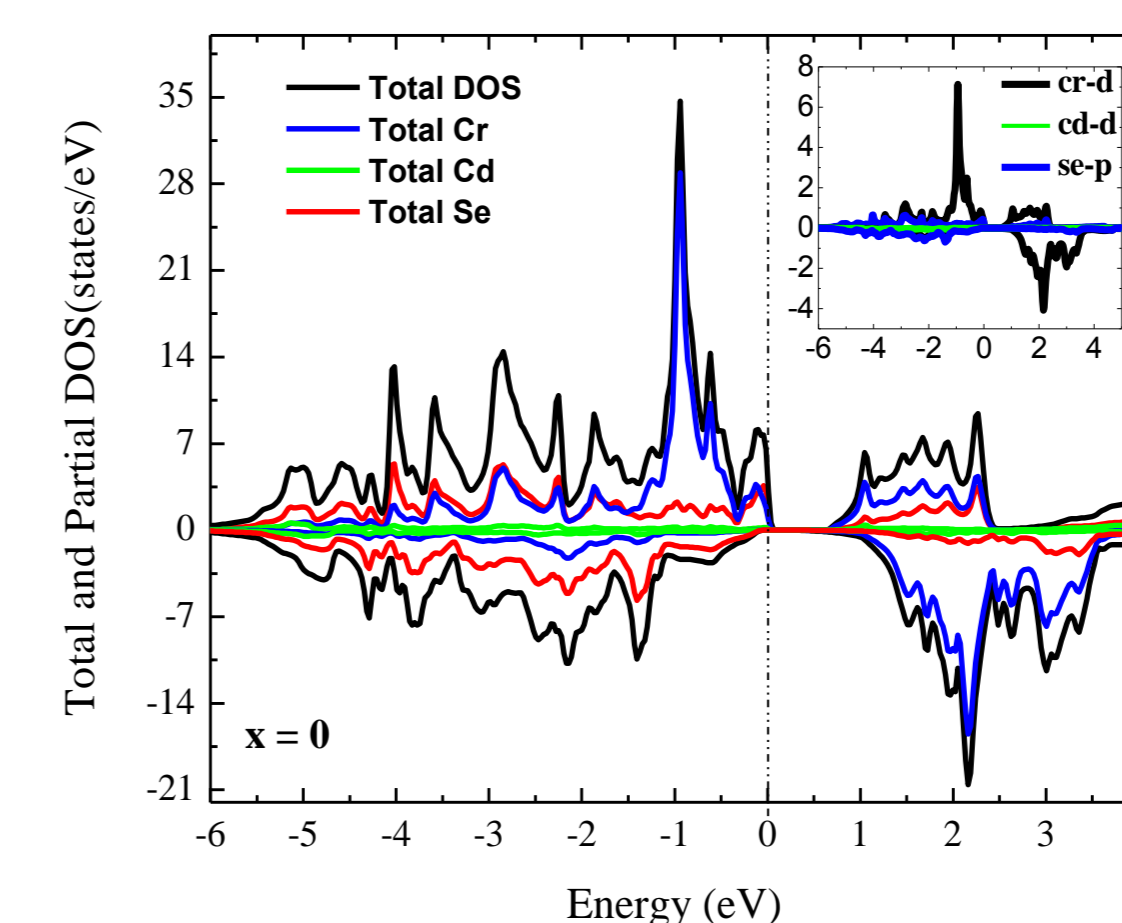
Figure 3: Total density of state (DOS) of $CdCr_2Se_4$ spinel computed with GGA approach, inset shows the partial densities of electronic states for Cr-3d, Cd-3d and Se-4p.
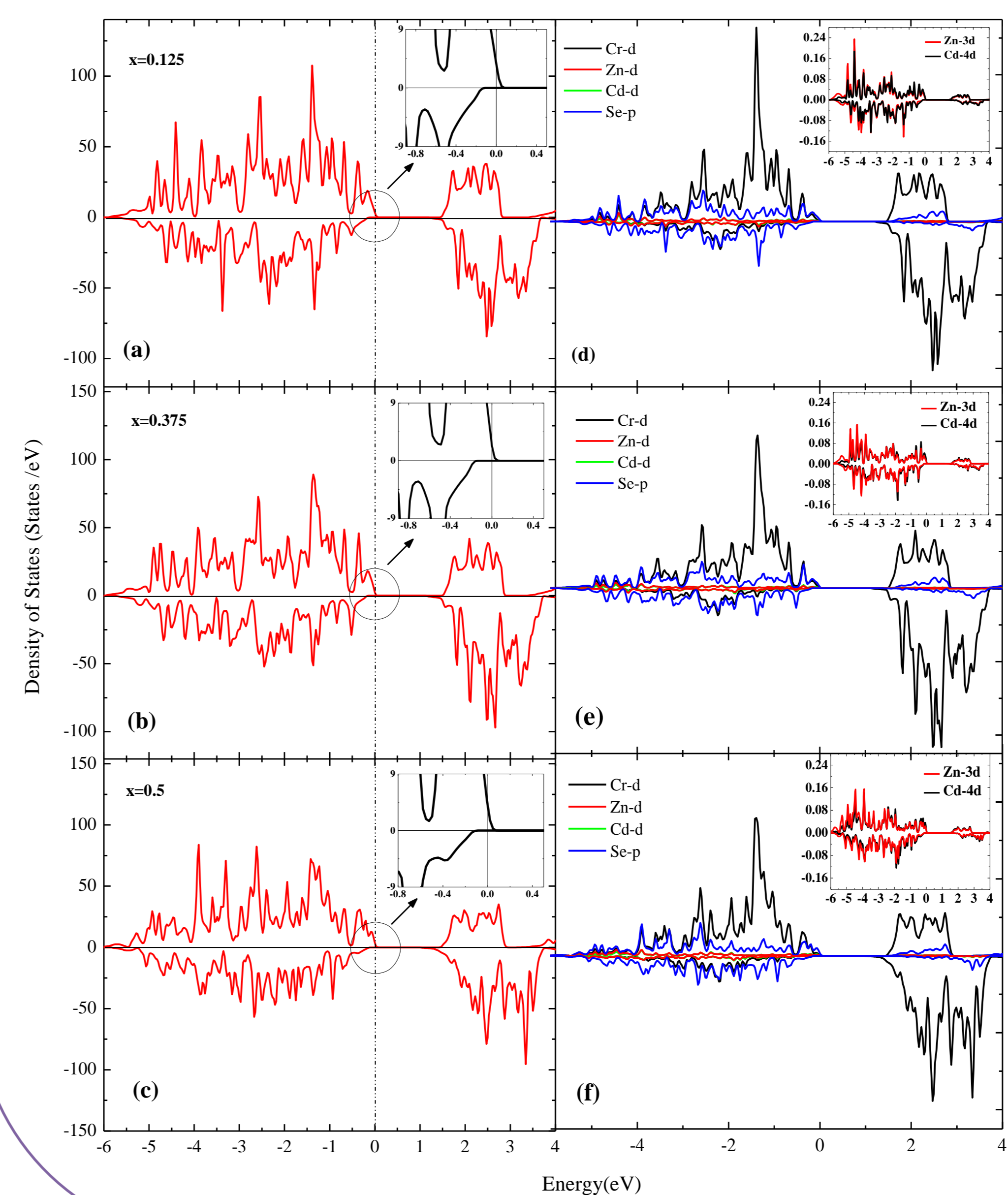
➤ Figure 1 displays the magnetic field dependence of the magnetization up to 15 T and temperature for $Cd_{1-x}Zn_xCr_2Se_4$ with (x=0.35, 0.45 and 0.55) at 4.2 K. Sample x=0.35 and x=0.45 exhibit a ferromagnetic behavior, while sample x=0.55 shows a spin glass like behavior due to the ferromagnetic FM and antiferromagnetic AFM competition that increases with increasing Zn content.

➤ The magnetic moment of Cr (μ_{Cr}) was found to decrease and scale linearly with increasing Zn concentration from 2.99 to 2.94 μ_B for *x* varying from 0.0 to 0.5 pointing out a small degradation of ferromagnetism

➤ The asymmetry in total density of state (DOS) deduced from band structure calculation for $CdCr_2Se_4$ (Figure 3) confirms the marked magnetic character. The low value gap close to Fermi level E_F demonstrates the semiconductor character. From the partial DOS (figure 3-inset) one can deduce the larger contribution of the Cr atom highlighting that the major contribution to the magnetization is associated to Cr.

Table 1 Variation of Curie temperature, spontaneous magnetization, magnetic moment of Cr calculated experimentally left) $Cd_{1-x}Zn_xCr_2Se_4$(x= 0.35, 0.45 and 0.55) and theoretically with GGA (right) (x=0, 0.125, 0.375 and 0.5).

Compound	T_C (K)	M (emu/g)	Magnetic moment (μ_B/Cr.at) Experimental		Magnetic moment (μ_B/Cr.at) Theoretical
$Cd_{1-x}Zn_xCr_2Se_4$					
x=0	129 [8]	59.00	2.81±0.05 [26,27]	x=0	2.992
x=0.35	74	61.03	2.82±0.05	x=0.125	2.980
x=0.45	54	61.23	2.80±0.05	x=0.375	2.961
x=0.55	40	62.57	2.83±0.05	x=0.5	2.948

6- Corrected gap energy

The total density of states of the $Cd_{1-x}Zn_xCr_2Se_4$ spinel was performed based on the FP-LAPW method using the popular GGA, however it is difficult to obtain satisfactory electronic structure and related properties for this latter because band gap energy is underestimated. Therefore, we have used the modified Beck-Johnson (mBJ) exchange potential approximation as a correction to the GGA. The combination of mBJ exchange and GGA correlation can produce accurate semiconductor gaps because it improves the d-state positions. The corresponding density of states between -6 and 4 eV were plotted in Figure 4. The gap energy calculated with mBJ was larger than that obtained with GGA for all Zn concentrations, the GGA + mBJ gap was found to be 1.11 eV and does agree with the experimental gap 1.15 eV (Table 2). Figures 4 (d-f) show the partial DOS of the Cr-d, Zn-d, Cd-d and Se-p bands.

Zn content	Lattice parameter (Å)	Gap Energy (eV) Theoretical GGA	Gap Energy (eV) Experimental	Gap Energy (eV) Theoretical mBJ
x=0	10.736	0.376 - 0.43 [29]	1.15 [29]	1.11
x=0.125	10.707	0.628	----	1.30
x=0.375	10.649	0.535	----	1.22
x=0.50	10.620	0.490	----	1.18

Table 2 The energy gaps (eV) calculated with GGA and with mBJ approach with the corresponding experimental values and lattice parameter for $Cd_{1-x}Zn_xCr_2Se_4$ (x= 0, 0.125, 0.375 and 0.5).

8- Total energy difference

The positive value of ΔE demonstrates that the FM configuration is more stable than the AFM interaction. Figure 6 displays the change of ΔE as a function of Zn content. ΔE present a positive trend in all concentrations, confirming that the FM is more dominant than that of the AFM one for all samples. Nevertheless, the values of ΔE are very small (10^{-4} Ry) pointing out a strong competition between the FM and AFM interactions. ΔE decreases with increasing Zn concentration, indicating that the AFM contribution slightly increases.

7- Exchange integrals

Figure 6 Calculated $ΔE = E_{AFM}-E_{FM}$ (Ry) as a function of Zn content for $Cd_{1-x}Zn_xCr_2Se_4$ spinels.
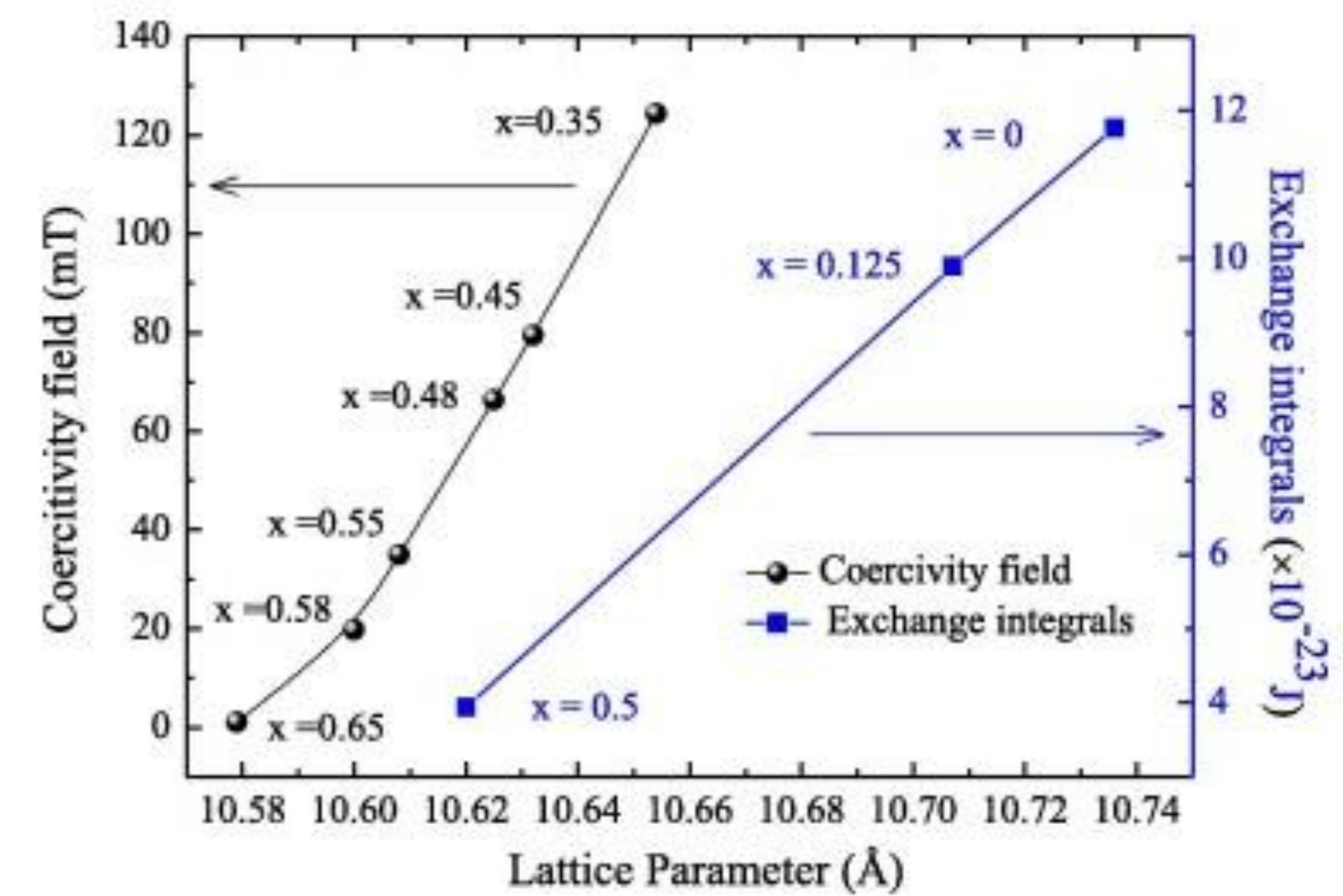

To investigate more the magnetic behavior, we calculated the exchange integrals using mean field approximation that gives the relation between the exchange integral J and the paramagnetic Curie temperature:

$$J_{ij} = \frac{3\, \theta_p k_B}{2\, S(S+1)Z}$$

Where $S=3/2$ is the Cr spin number and Z represents the first nearest neighbors of Cr ($Z=6$), is the paramagnetic Curie temperature and k_B is the Boltzmann constant. Using our , we plotted the change of J as a function of Zn content in Figure 5. The decrease of the exchange integrals is due to decrease of lattice parameter (Table 2) that enhances the magnetic competition between ferromagnetic and antiferromagnetic states by super-exchange mechanics, which explains the small decrease of magnetic moment with Zn substitution (Table 1). To support the increase of antiferromagnetic contribution with increasing Zn content, we have calculated the difference in energy between AFM and FM configurations $ΔE = E_{AFM} - E_{FM}$ using *ab*-initio calculations. The positive value of ΔE demonstrates that the FM configuration is more stable than the AFM interaction

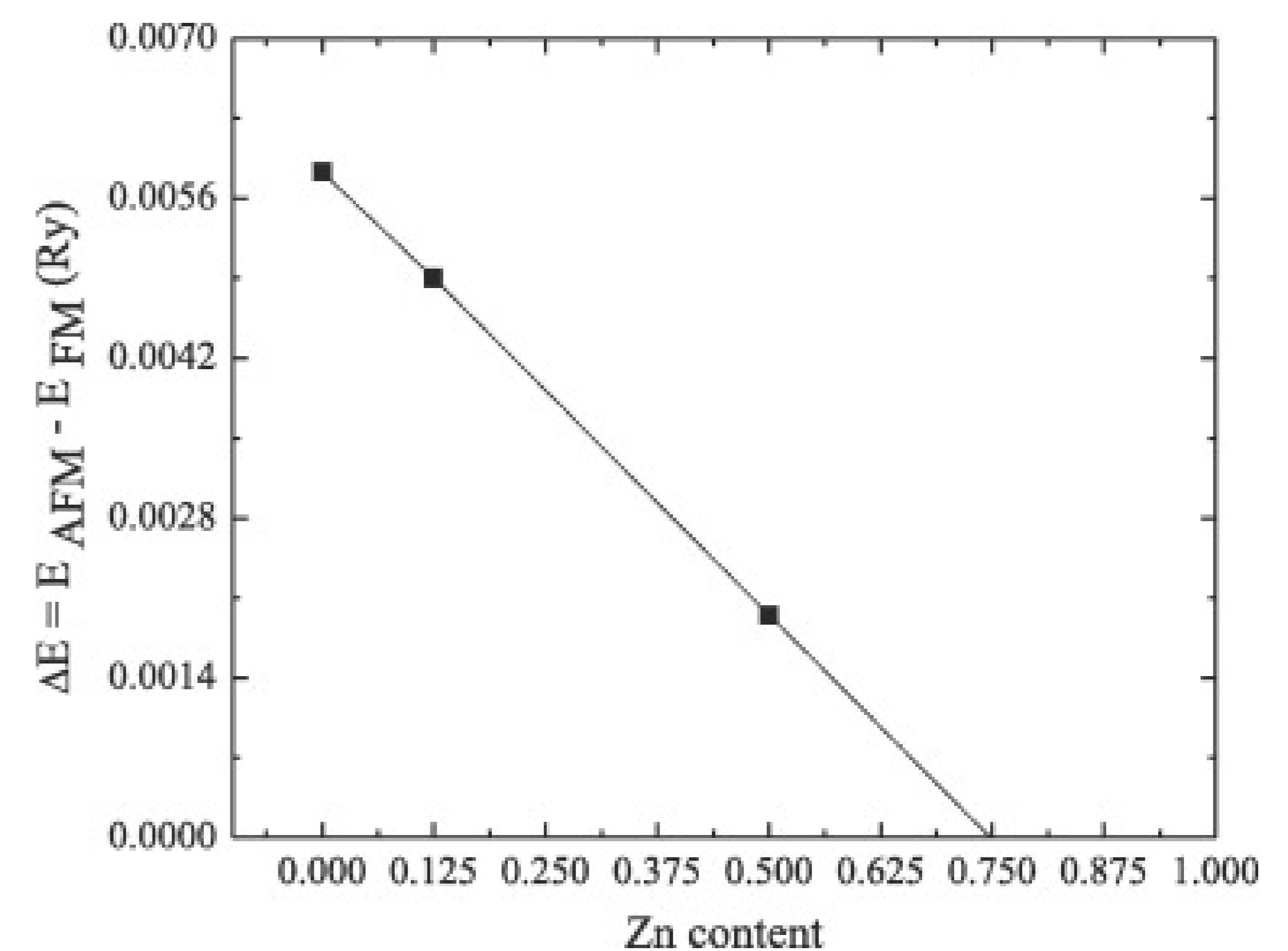## Conclusion

In summary, using *ab*-initio calculations based on GGA and the improved DFT method mBJ, the magnetic and electronic properties of the quaternary $Cd_{1-x}Zn_xCr_2Se_4$ ($0 \leq x \leq 0.5$) spinels were investigated. The asymmetrical nature of density of states indicates the magnetic behavior for all samples. The band gaps calculated from the GGA+mBJ approach agree more with the experimental data. It is found that Zn substitution enhances the AFM contribution raised from super-exchange interactions while the FM state keeps the dominance in this range ($0 \leq x \leq 0.5$) with a non-negligible competition between both states. It is found that the spinel system keeps the half-metallicity behavior for all through substitution with 100% spin polarization. Finally, these results are helpful to comprehend the magnetism and electronic structure in Zn-substituted $Cd_{1-x}Zn_xCr_2Se_4$ semiconductors and predict its application in spintronic technology.

Laboratoire de Physique des Matériaux, Microélectronique, Automatique et Thermique (LPMMAT)
Adresse: Département de physique Faculté des Sciences Ain Chock B.P 5366 Maarif Casablanca 20100 Maroc
Tél: 00 212 522 23 06 80 / 84   Fax: 00 212 522 23 06 74